

## T-cell triggering thresholds are modulated by the number of antigen within individual T-cell receptor clusters

Boryana N. Manz<sup>1,4</sup>, Rebecca S. Petit<sup>2,4</sup>, Bryan L. Jackson<sup>2,4</sup>, Michael L. Dustin<sup>3</sup>, Jay T. Groves<sup>1,2,4,5</sup>

<sup>1</sup> Biophysics Graduate Group, <sup>2</sup> Department of Chemistry, University of California at Berkeley, Berkeley, CA 94720, USA. <sup>3</sup> Program in Molecular Pathogenesis, Skirball Institute of Biomolecular Medicine and Department of Pathology, New York University School of Medicine, New York, NY 10016, USA. <sup>4</sup> Physical Biosciences and Materials Sciences Divisions, Lawrence Berkeley National Laboratory, Berkeley, CA 94720, USA. <sup>5</sup> Howard Hughes Medical Institute

Correspondence should be addressed to JTG at [JTGroves@lbl.gov](mailto:JTGroves@lbl.gov)

### Abstract

Spatial organization of T cell receptors (TCR) into clusters upon engagement of their peptide major histocompatibility complex (pMHC) ligands is essential for T cell activation. T cells are known to react to extremely small numbers of activating agonist peptides, however quantitative and accurate determination of the minimal triggering unit has proven to be extremely difficult. Here we have designed an experimental strategy that enables direct control over the number of agonist peptides per TCR cluster, without altering the total number engaged by the cell. A key observation from these experiments is that the threshold for triggering calcium flux is determined by the number of activating ligands within individual TCR clusters; it is not determined by the total number encountered by the cell. Results from a series of experiments in which agonist density and TCR cluster size are independently and controllably varied in primary T cells indicate that triggering occurs when the average number of a activating pMHC per TCR cluster is  $\sim 2$ . However, a stochastic analysis of activating pMHC distribution among clusters suggests the most probable minimal triggering unit may contain 4 – 6 agonist per cluster.

### Introduction

T cells exhibit an exquisite ability to recognize extremely low densities of agonist peptide antigen displayed in major histocompatibility complex proteins on the surface of antigen presenting cells. Some studies have suggested that T cells may react to even a few individual agonist peptide molecules<sup>1,2</sup>. Additionally, T cells maintain this extreme sensitivity without spontaneous triggering in the absence of agonist, which would lead to autoimmune disorders<sup>3,4</sup>. Various mechanisms for how high sensitivity to agonist with apparent immunity to stochastic noise have been proposed; these generally rely on cooperativity among multiple receptors and signaling molecules within the TCR-pMHC clusters<sup>4-16</sup>. However, the specific physical mechanisms by which these remarkable

capabilities are achieved remain unresolved, due largely to experimental limitations. Key to ultimately determining, and experimentally verifying, the molecular mechanism of TCR triggering is to gain direct control over TCR cluster assembly and peptide ligand composition in living T cells.

In the following, we present results from experiments that directly probe the consequences of differentially partitioning agonist peptide among TCR clusters in primary T cells. The strategy is based on the hybrid live cell – supported membrane configuration, in which a solid supported lipid bilayer takes the place of the antigen presenting cell<sup>17-19</sup>. Histidine-tagged variants of MHC class II and intercellular adhesion molecule-1 (ICAM-1) are linked to the membrane through Ni<sup>2+</sup>-chelating lipid groups<sup>19,20</sup>. The proteins diffuse freely and as monomers on the supported membrane (See supporting information). MHC density on the membrane surface as well as peptide composition are thus under direct experimental control. Control over TCR clustering is achieved through grid patterns of metal lines, which have been prefabricated onto the underlying solid substrate. These structures, known as diffusion or mobility barriers<sup>17,21-23</sup>, block lateral transport of lipids and supported membrane associated proteins. Molecules continue to diffuse freely within each corral, but are unable to hop between separate corrals. As the TCR engage pMHC, clustering ensues until all pMHC within a single corral of the grid partitioned supported membrane are coalesced into a single cluster with their cognate TCR receptors. The number of pMHC within each supported membrane corral determines the size of TCR signaling clusters on the T cell. Thus adjusting the grid size at constant pMHC density enables titration of TCR cluster size without changing the number of antigen engaged by the T cell. We refer to this mechanical manipulation of molecular spatial organization within living cells as a spatial mutation<sup>17,24</sup>. In the present application, chemically identical T cells differing only in the size distribution of their TCR clusters are generated.

The primary goal of the present study is to determine what is the minimal signaling unit sufficient for antigen pMHC to trigger Ca<sup>2+</sup> flux in T cells. We perform a two parameter titration experiment in which the overall antigen peptide surface density as well as its partitioning among TCR clusters are independently controlled in living T cells. The results clearly indicate that threshold antigen densities for triggering Ca<sup>2+</sup> flux are dependent on TCR cluster size. Most significantly, when these antigen dose-response functions are renormalized in terms of the number of antigen per cluster, they collapse onto a single curve. T cells trigger at an average agonist density of ~2 per TCR cluster, irrespective of the total number of agonist pMHC engaged by the cell. Interpretation of this invariant activation response in terms of the Poisson distribution of agonist pMHC among TCR clusters indicates the most likely activation threshold is 4 – 6 antigenic peptides within a single TCR cluster. The implications of these measurements with respect to the mechanism of TCR signaling are discussed.

## Results

### *Physical partitioning of T cell receptor clusters*

T cell activation is investigated in a hybrid immunological synapse consisting of primary mouse T cells interacting with functionalized supported lipid bilayer membranes (Fig.1a). This configuration is widely used and has been instrumental in characterizing the immunological synapse<sup>13,17,18</sup>. The supported membranes are formed by spontaneous assembly from small unilamellar vesicles on glass substrates. A characteristic feature of supported membranes, which is critical for these experiments, is the free lateral mobility of membrane associated lipids and proteins<sup>20,25,26</sup>. For hybrid immunological synapse reconstitution, the supported membrane is functionalized with ICAM-1 and MHC loaded with agonist (MCC) or null (T102E) peptide<sup>13,17,18</sup>. The cytoplasmic domains of these proteins are expressed as histidine-tag constructs (his10 and 2Xhis6, respectively) and stably linked to the supported membrane by multivalent interactions with Ni<sup>2+</sup>-chelating lipids doped into the membrane; we employ kinetic control parameters to achieve desired densities of bound protein<sup>19,20</sup>.

AND TCR effector T cells form hybrid junctions with these supported membranes irrespective of the peptide displayed by MHC. When all of the MHC is loaded with T102E peptide, T cells spread on the surface and exhibit a relatively homogeneous distribution of TCR (Fig. 1b). At low concentrations of MCC-MHC, TCR organize into clusters throughout the contact zone. At much higher MCC-MHC, these TCR clusters are actively driven towards the center of the interface by an actin polymerization dependent process, forming the classical immunological synapse pattern (Fig.1 b,c)<sup>13,27</sup>.

Physical structures on the underlying supported membrane substrate can be used to control TCR clustering in the living cell. Barriers to lateral mobility of supported membrane components are created by grid patterns of metal lines (5nm high, 100nm wide) that are prefabricated onto the glass substrate by electron beam lithography. Grid patterns trap fixed numbers of pMHC and ICAM-1 within each confined grid corral, without otherwise interfering with their mobility.. As TCR engage these mobile but trapped pMHC, they also become subject to the substrate-imposed constraint. Generally, we observe all pMHC-TCR within a single corral to assemble into one microcluster; the number of MHC per corral thus directly determines TCR cluster size. Other molecules on the T cell not interacting directly with MHC or ICAM-1 in the supported bilayer move freely throughout the entire interface. As examples, actin and CD45 are successfully transported to the center of the immunological synapse irrespective of constraint patterns (Supplemental Fig. 1 a,b).

*Partitioning of agonists among TCR clusters alters the threshold density to trigger intracellular calcium flux*

The experimental ability to independently control TCR cluster size and pMHC density enables characterization of TCR cluster signaling with unprecedented specificity. A typical experiment is depicted in Fig. 2. A population of identical T cells is allowed to interact with a supported membrane that is partitioned by substrate patterns in one region and unpartitioned elsewhere. T cell triggering is monitored by intracellular  $\text{Ca}^{2+}$  flux using fluorescence ratio imaging of fura-2 dye (Fig. 2a)<sup>18,28</sup>. The supported membrane is of uniform composition over the entire substrate. Thus differences in T cell triggering on and off patterned regions results exclusively from differences in pMHC-TCR cluster size. These experiments are performed at overall pMHC density of  $100 \mu\text{m}^{-2}$ . If all the peptides are the MCC agonist at these densities, robust intracellular  $\text{Ca}^{2+}$  flux is observed at all cell grid sizes<sup>17</sup>. As MCC is diluted with T102E null, threshold densities for triggering can be identified.

There are several reasons for titrating agonist:null peptide ratio rather than total MHC. First, under physiological conditions T cells generally encounter relatively high MHC density and must search for rare agonist peptides. Second, molecules are stochastically distributed (Poisson) among the supported membrane corrals and the standard deviation of these random distributions is  $\sqrt{N}$ , where  $N$  is the average number of molecules per corral. A more uniform MHC distribution is thus achieved at higher densities. Specific effects of the stochastic distribution of dilute MCC agonist peptide must still be considered; these are intrinsic to TCR signaling and are discussed further below.

Quantitative results from a representative TCR cluster size titration experiment are illustrated in Figure 2 b,c. This experiment was performed with an overall MCC-MHC density of  $8.6 \mu\text{m}^{-2}$ . At this density, similarly high fractions of cells triggered on  $1 \mu\text{m}$  grids, as did off. By contrast  $0.5 \mu\text{m}$  grid partitioning effectively blocked activation. Note that the barrier line width is not negligible and must be accurately measured by scanning electron microscopy and quantitative fluorescence (see supporting information) to calculate correct membrane area in different grid sizes. Patterns consisting of a non-percolating arrays of solid squares with similar area coverage as the grids do not partition TCR clusters and yield similar activation ratios as observed off patterns. This control experiment provides critical confirmation that the presence of metal on the substrate does not appreciably alter T cell response.

By partitioning TCR clusters more finely with the  $0.5 \mu\text{m}$  grids, triggering was essentially turned off without changing the total number of agonist pMHC engaged by the cell. Thus, the minimum agonist density recognized by T cells depends on how TCR are clustered. From this observation, we may also conclude that, at the very least, a single agonist pMHC per TCR cluster is insufficient to trigger.

### *Minimal number of agonist per signaling TCR cluster*

One is not enough, but what is the minimum number of agonist pMHC per TCR cluster sufficient for triggering? We explore this question through a series of experiments in which agonist pMHC density is titrated on different grid sizes. As seen in Figure 3a the activation density for triggering  $\text{Ca}^{2+}$  flux becomes progressively higher as grid size and TCR cluster size, get smaller. If these data are instead plotted in terms of the number of agonist pMHC per cluster, then the 1  $\mu\text{m}$  and 0.5  $\mu\text{m}$  activation curves collapse to a single dose-response function (Figure 3b). We observe the TCR triggering when the average number of agonist pMHC per TCR cluster reaches  $\sim 2$ . The fact that there are more TCR clusters in the more finely partitioned cells does not affect this threshold. Additional increases in  $\text{Ca}^{++}$  triggering as MCC-MHC density increases further are much more gradual. The onset of triggering occurs abruptly once a critical number of agonist pMHC per TCR cluster is reached.

At such low densities, the stochastic distribution of agonist pMHC among the many TCR clusters in each cell must also be considered. In our experimental procedure, both agonist and null peptides are exposed to membrane-associated MHC from solution simultaneously. Therefore we expect uncorrelated loading of both peptides. This results in a Poisson distribution for the number of MCC peptides in each TCR cluster. The Poisson distribution for the probability of a given TCR cluster having a particular number of MCC-MHC for different average numbers of MCC-MHC per cluster is plotted in Figure 3c.

Next, we compare the Poisson distribution at an average MCC-MHC density of 1 per cluster, which was not activating, to an MCC-MHC density of 2 per cluster, which was activating, as traced by grey lines between figures 3 b and c. Notice that the probability of 2 MCC-MHC in a single cluster is relatively unchanged and the probability of 2 or more changes by less than two-fold between the non-activating and activating situations. In contrast, the number of TCR clusters with 3 and, to an even greater extent, 4 MCC-MHC has risen sharply. From these results, one is forced to conclude that the most probable minimal triggering unit is at least 4 agonist per TCR cluster and could be as high as 6. It is unlikely that 7 or more agonist are required since the probability of these becomes so low that many cells would have no TCR clusters with this many agonist.

### **Discussion**

Some consideration is required to rectify the difference between the measured minimum triggering threshold based on average and stochastic analyses. First, we note that triggering as defined by intracellular  $\text{Ca}^{++}$  flux is essentially digital. Onset of  $\text{Ca}^{++}$  flux is abrupt and does not exhibit a graded response at low antigen densities. The next question then concerns whether individual TCR clusters trigger with an all-or-nothing or a graded response. Speculation on this matter abounds, but based on the experimental

evidence reported here it is unlikely TCR clusters could yield a graded response. We arrive at this conclusion based on the fact that partitioning TCR clusters at a constant total amount of antigen leads to an abrupt cessation of triggering. If multiple partially-triggered TCR clusters were somehow integrated within the cell to yield the equivalent of one fully triggered cluster, then such discrete changes as a function of partitioning alone are not expected. Our results are most consistent with a mechanism in which individual TCR clusters trigger, all-or-nothing, based on achieving some minimum threshold.

Within this model, the probability of a TCR cluster triggering will be a function of the number of agonist in the cluster. However, it is not necessary that a specific threshold number of agonist per cluster, above which the cluster always triggers and below which it never does, even exist. Rather, all we can expect is that the probability of a cluster triggering increases with agonist number and that this increase may be particularly abrupt around a certain critical number of agonist per cluster. Our experimental results suggest that no such abrupt increase occurs for clusters with only two agonists. Instead, abrupt increases in the probability of triggering intracellular  $\text{Ca}^{++}$  flux occur in correlation with the appearance of TCR clusters containing four agonist pMHC. Direct coupling of two TCRs, by bivalent antibody or agonist dimers, has been shown to trigger T cells<sup>7,9</sup>. These well known facts, along with structural evidence, naturally lead to the assumption that a TCR dimer is the fundamental triggering unit. However the artificial tether between agonists alters the dynamics of agonist-TCR and TCR-TCR association, possibly stabilizing it beyond physiological conditions and therefore cannot reveal the complete mechanism of signaling. The experimental design used here does not enforce or require direct dimerization between agonist-MHCs.

In conclusion, the TCR cluster size titration experiments described here arguably constitute the most quantitative analysis of TCR triggering sensitivity to date. The results are generally consistent with the extreme, near-single-molecule, sensitivity of T cells to antigen long thought to exist. Cluster size titration further reveals that spatial organization into TCR clusters is critical to achieve this sensitivity. The observation that 4 antigen per cluster is a more likely candidate as a minimal triggering unit than a dimer raises interesting questions concerning large-scale cooperativity in receptor signaling clusters.

## **Methods summary**

AND TCR effector cells were generated and used on day 5 and 7<sup>17</sup>. Supported lipid bilayer membrane, doped with 2% mol  $\text{Ni}^{2+}$ -chelating lipids, was reloaded with  $\text{NiCl}_2$  and functionalized with his-MHC (I-E<sup>k</sup>) (preloaded with different ratios of agonist MCC and null T102E peptide) and ICAM-1<sup>19</sup>. Cells were loaded with fura-2-AM dye, injected in pre-warmed to 37°C flow chamber are imaged every 7 or 15 sec<sup>17</sup>. MHC surface density was measured by quantitative fluorescence of Alexa Fluor® conjugated peptide, and calibrated with supported bilayer with known molar concentration of a fluorescent species<sup>30</sup>.

Chromium lines were fabricated by two-layer liftoff process with e-beam lithography and verified by scanning electron microscopy at UC Berkeley Microfabrication lab and Molecular Foundry, LBNL.

Complete material and methods and supplementary information is available.

### **Acknowledgements**

The authors would like to acknowledge Andrew DeMond, Nina Hartman, Joseph Hickey and Jeff Nye for experimental reagents, and the Molecular Foundry, LBNL for substrate preparation. Work at the Molecular Foundry was supported by the Office of Science, Office of Basic Energy Sciences, of the U.S. Department of Energy under Contract No. DE-AC02-05CH11231.

### **Author contributions**

BNM, MLD and JTG designed research, BNM, BLJ, RSP and MLD supplied essential reagents and substrates, BNM performed experiments, BNM analyzed data, BNM and JTG wrote the manuscript.

## References (max 30)

1. Irvine, D. J., Purbhoo, M. A., Krogsgaard, M. & Davis, M. M. Direct observation of ligand recognition by T cells. *Nature*. **419**, 845-9 (2002).
2. Stefanova, I., Dorfman, J. R. & Germain, R. N. Self-recognition promotes the foreign antigen sensitivity of naive T lymphocytes. *Nature*. **420**, 429-34 (2002).
3. Wylie, D. C., Das, J. & Chakraborty, A. K. Sensitivity of T cells to antigen and antagonism emerges from differential regulation of the same molecular signaling module. *Proc Natl Acad Sci U S A*. **104**, 5533-8 (2007).
4. Li, Q. J. *et al.* CD4 enhances T cell sensitivity to antigen by coordinating Lck accumulation at the immunological synapse. *Nat Immunol*. **5**, 791-9 (2004).
5. Bray, D., Levin, M. D. & Morton-Firth, C. J. Receptor clustering as a cellular mechanism to control sensitivity. *Nature*. **393**, 85-8 (1998).
6. Boniface, J. J. *et al.* Initiation of signal transduction through the T cell receptor requires the multivalent engagement of peptide/MHC ligands [corrected]. *Immunity*. **9**, 459-66 (1998).
7. Cochran, J. R., Cameron, T. O. & Stern, L. J. The relationship of MHC-peptide binding and T cell activation probed using chemically defined MHC class II oligomers. *Immunity*. **12**, 241-50 (2000).
8. Chakraborty, A. K. Lighting up TCR takes advantage of serial triggering. *Nat Immunol*. **3**, 895-6 (2002).
9. Krogsgaard, M. *et al.* Agonist/endogenous peptide-MHC heterodimers drive T cell activation and sensitivity. *Nature*. **434**, 238-43 (2005).
10. Schamel, W. *et al.* Coexistence of multivalent and monovalent TCRs explains high sensitivity and wide range of response. *J Exp Med*. **202**, 493 - 503 (2005 Aug 15).
11. Alarcon, B., Swamy, M., van Santen, H. M. & Schamel, W. W. T-cell antigen-receptor stoichiometry: pre-clustering for sensitivity. *EMBO Rep*. **7**, 490-5 (2006).
12. Bunnell, S. C. *et al.* Persistence of cooperatively stabilized signaling clusters drives T-cell activation. *Mol Cell Biol*. **26**, 7155-66 (2006).
13. Varma, R. *et al.* T cell receptor-proximal signals are sustained in peripheral microclusters and terminated in the central supramolecular activation cluster. *Immunity*. **25**, 117-27 (2006).
14. Hlavacek, W. S. *et al.* Kinetic proofreading models for cell signaling predict ways to escape kinetic proofreading. *Proc Natl Acad Sci U S A*. **98**, 7295-300 (2001).
15. Seminario, M. C. & Bunnell, S. C. Signal initiation in T-cell receptor microclusters. *Immunol Rev*. **221**, 90-106 (2008).
16. Coombs, D. *et al.* Activated TCRs remain marked for internalization after dissociation from pMHC. *Nat Immunol*. **3**, 926-31 (2002).
17. Mossman, K. D., Campi, G., Groves, J. T. & Dustin, M. L. Altered TCR signaling from geometrically repatterned immunological synapses. *Science*. **310**, 1191-3 (2005).
18. Grakoui, A. *et al.* The immunological synapse: a molecular machine controlling T cell activation. *Science*. **285**, 221-7 (1999).



19. Nye, J. A. & Groves, J. T. Kinetic control of histidine-tagged protein surface density on supported lipid bilayers. *Langmuir*. **24**, 4145-9 (2008).
20. Groves, J. T. & Dustin, M. L. Supported planar bilayers in studies on immune cell adhesion and communication. *J Immunol Methods*. **278**, 19-32 (2003).
21. Groves, J. T., Ulman, N. & Boxer, S. G. Micropatterning fluid lipid bilayers on solid supports. *Science*. **275**, 651-3 (1997).
22. Groves, J. T. & Boxer, S. G. Micropattern formation in supported lipid membranes. *Acc Chem Res*. **35**, 149-57 (2002).
23. Jackson, B. L., Nye, J. A. & Groves, J. T. Electrical manipulation of supported lipid membranes by embedded electrodes. *Langmuir*. **24**, 6189-93 (2008).
24. Groves, J. T. Spatial mutation of the T cell immunological synapse. *Curr Opin Chem Biol*. **10**, 544-50 (2006).
25. Sackmann, E. Supported membranes: Scientific and practical applications. *Science*. **271**, 43-48 (1996).
26. Groves, J. T., Wulfing, C. & Boxer, S. G. Electrical manipulation of glycan-phosphatidyl inositol-tethered proteins in planar supported bilayers. *Biophys J*. **71**, 2716-23 (1996).
27. DeMond, A. L. *et al.* T cell receptor microcluster transport through molecular mazes reveals mechanism of translocation. *Biophys J*. **94**, 3286-92 (2008).
28. Wulfing, C. *et al.* Kinetics and extent of T cell activation as measured with the calcium signal. *J Exp Med*. **185**, 1815-25 (1997).
29. Feinerman, O. *et al.* Variability and robustness in T cell activation from regulated heterogeneity in protein levels. *Science*. **321**, 1081-4 (2008).
30. Galush, W. J., Nye, J. A. & Groves, J. T. Quantitative fluorescence microscopy using supported lipid bilayer standards. *Biophys J*. **95**, 2512-9 (2008).

### Figure 1. Immunological synapse on partition patterns

**a.** Schematic of experimental strategy. Primary mouse T cells interact with MHC and ICAM-1 functionalized patterned supported lipid bilayer membrane. MHC is pre-loaded with null (T102E) or agonist (MCC) peptide. Chromium lines pre-fabricated on the glass are diffusion barriers to all lipids and lipid tethered proteins.

**b.** *En face* view of TCR distribution in the immunological synapse. Total internal reflection fluorescence (TIRF) images of anti-TCR fab on 0 MCC-MHC  $\mu\text{m}^{-2}$  (diffuse TCR), 1 MCC-MHC  $\mu\text{m}^{-2}$  (spread TCR clusters) and 100 MCC-MHC  $\mu\text{m}^{-2}$  (central TCR cluster). Image intensity is scaled to demonstrate clearly the TCR distribution in each case. Scale bar 5  $\mu\text{m}$ .

**c.** Percent of cells with the TCR distribution phenotypes in **b.** 10 min after contact with bilayer.  $n=140-150$  cells per concentration.

**d.** Bright field, reflection interference contrast microscopy (RICM), and TCR distribution of cells off grid, and on 3, 1, and 0.5  $\mu\text{m}$  side partition grids after 5-10 min of contact with the surface. TCR cluster until there is one TCR cluster per box. Scale bar 5  $\mu\text{m}$ .

### Figure 2. T cell activation on patterned partition grids

**a.** Bright field of T cells and grid (left) and false colored calcium levels (fura-2 ratio) (right). Top – off and on 0.5  $\mu\text{m}$  grid. Bottom – off and on 0.5  $\mu\text{m}$  control array. Small schematics of underlying patterns are overlaid in bright field image. The dashed line in the calcium images indicates the border between off and on grids. Calcium image 8:30 min after cell injection, bright field image ~30 min after cell injection. Scale bar 40  $\mu\text{m}$ .

**b.** Population calcium flux on partition grids. Bright field of representative cells on and off patterns (left) (scale bar 5  $\mu\text{m}$ ), schematic of agonist (MCC) and null (T102E) distribution in grid boxes (center) and false-colored calcium flux (fura-2 ratio) traces of >100 cells per region (right). Cell traces (each horizontal line is one cell) are ranked by their integrated calcium flux in descending order. Calcium is imaged every 15 sec.

**c.** Population mean ( $\pm$ sem) of integrated calcium flux on different size partition grids in **a** and **b**.

**a-c.** All data in this figure is from one representative experiment in one chamber with different patterns spaced ~0.3 mm apart. 8.6 MCC-MHC  $\mu\text{m}^{-2}$ .

### Figure 3. Partition titration of agonists per TCR cluster

**a.** T cell activation with respect to titration of overall MCC-MHC surface density off and on 1 and 0.5  $\mu\text{m}$  partition grids. The minimal density at which T cells activate is shifted higher from off grid (filled circle) to 1  $\mu\text{m}$  grid (open square), and even further to 0.5  $\mu\text{m}$  grid (crossed open box). Lines are guides to the eye. Mean calcium flux ( $\pm$  sem) of cells pooled from independent experiments per concentration.

**b.** T cell activation with respect to number of MCC-MHCs per box at 1  $\mu\text{m}$  (open box) and 0.5  $\mu\text{m}$  (open crossed box) partition grids. The transition to activation on

1 and 0.5  $\mu\text{m}$  grids is at the same number of MCC-MHC per box (between the two gray lines).

c. Theoretical Poisson distribution of the probability of discrete number of MCC-MHC per box at different average concentrations per box. At non-activating density (left gray line), most boxes have zero or one MCC-MHC. At activating densities (right gray line), an appreciable number of boxes have two MCC-MHCs.

**Figure 1.**

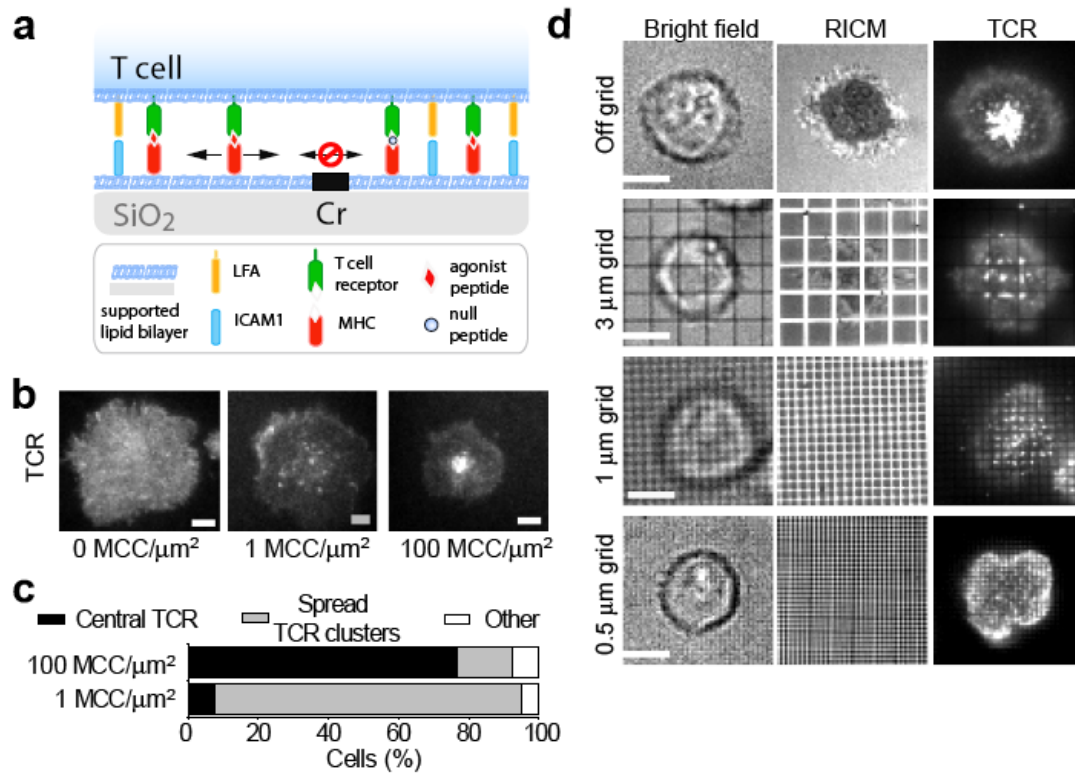


**Figure 2.**

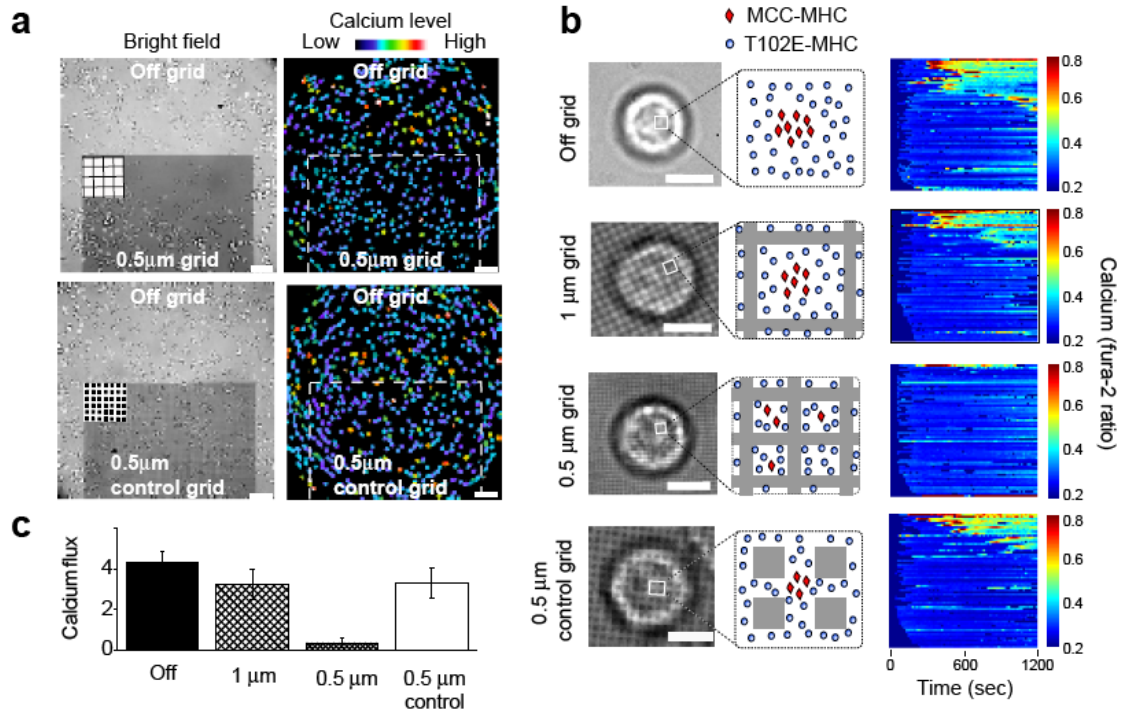
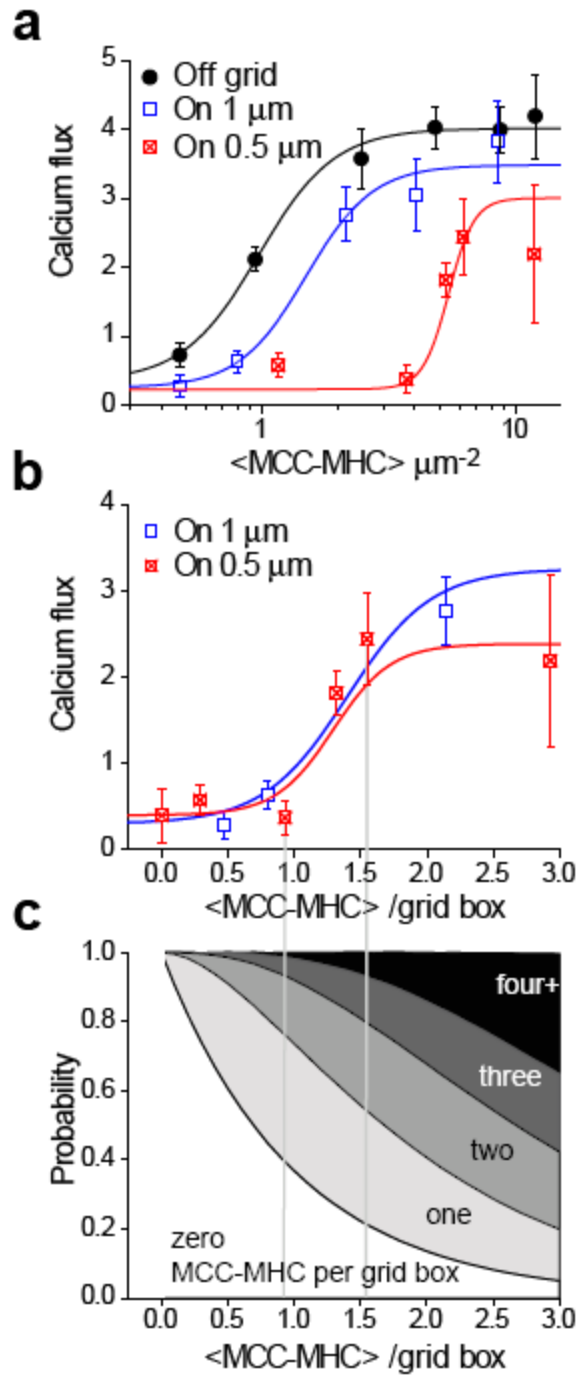
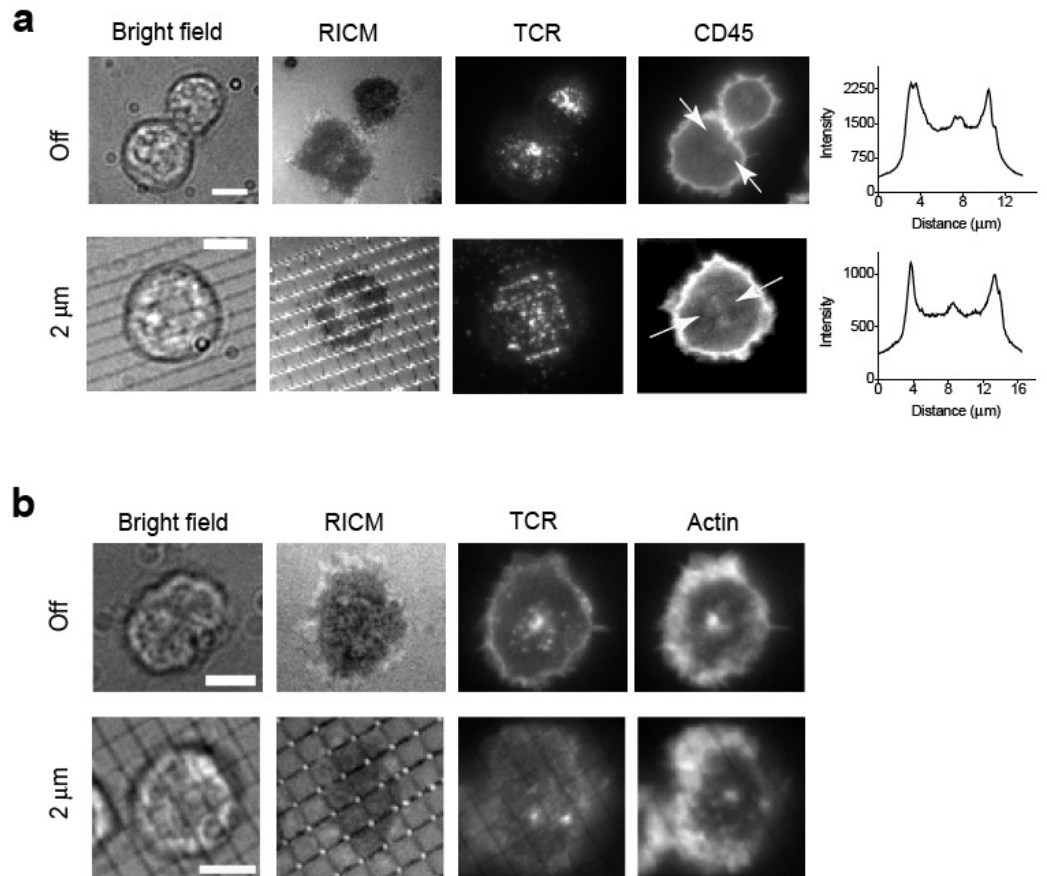


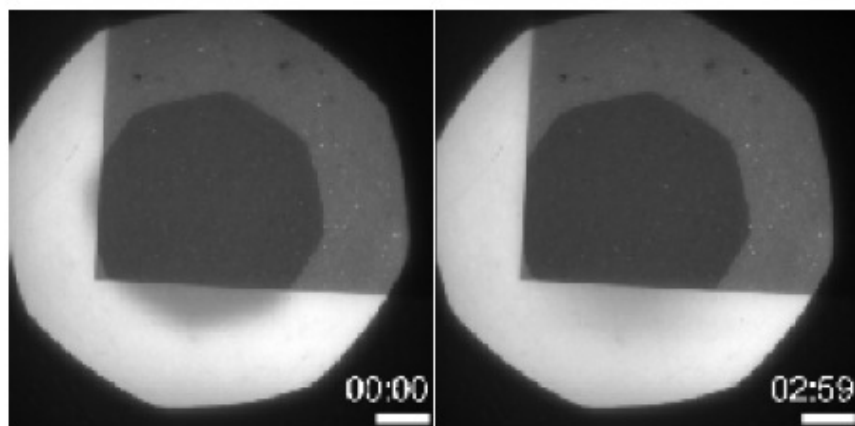
**Figure 3.**



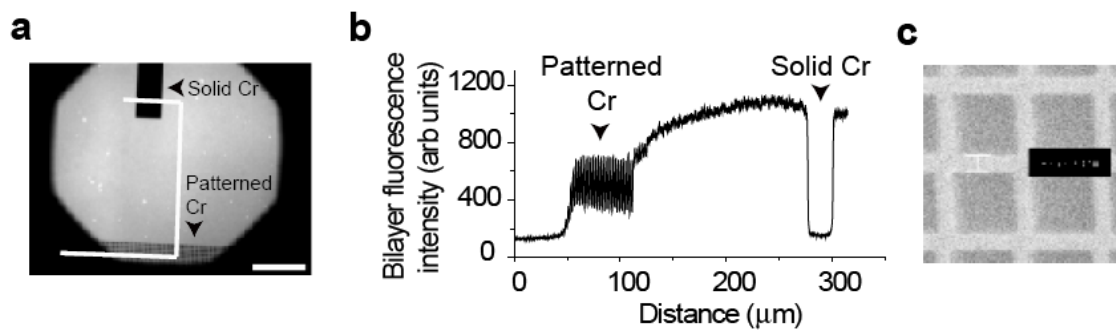
# Supplementary figure 1.



## Supplementary figure 2.

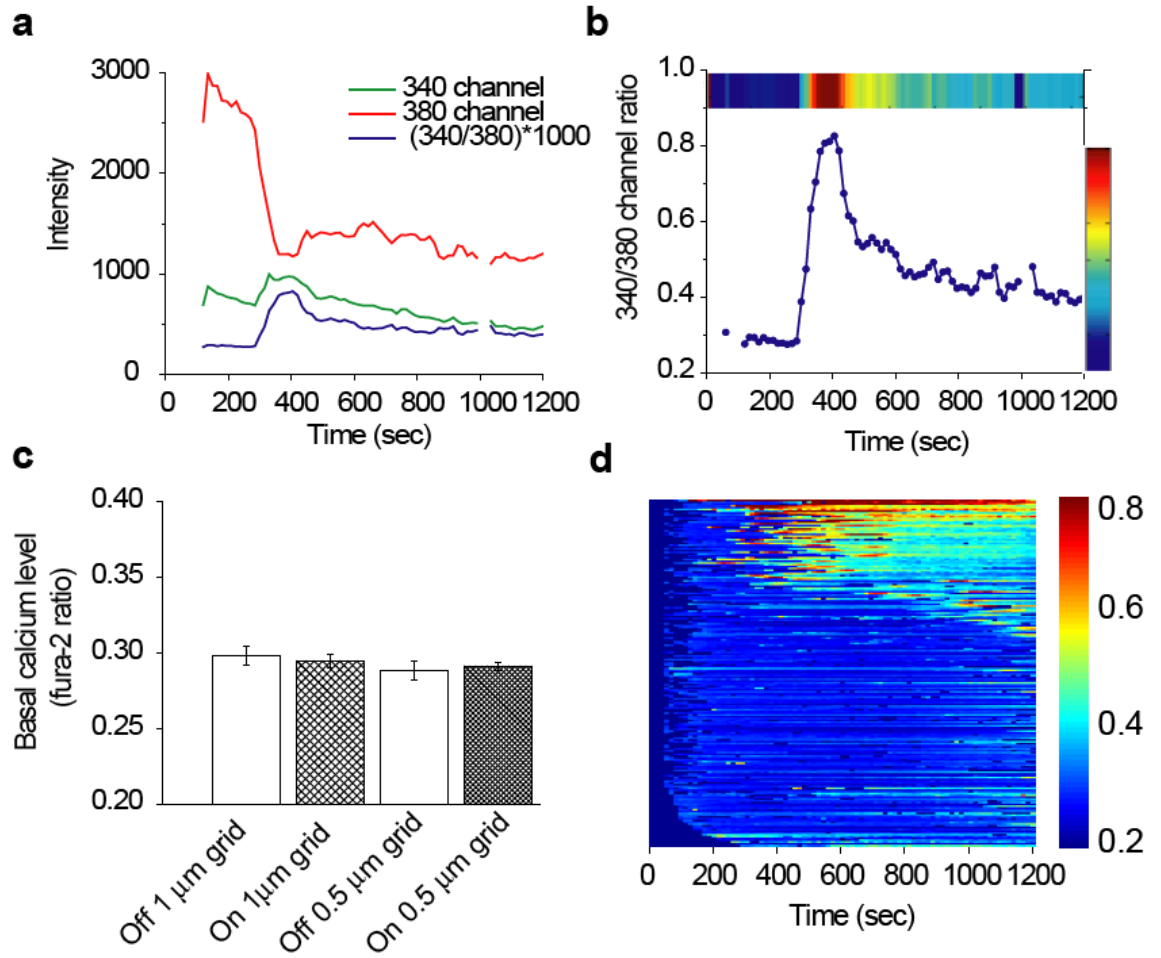


## Supplementary figure 3.



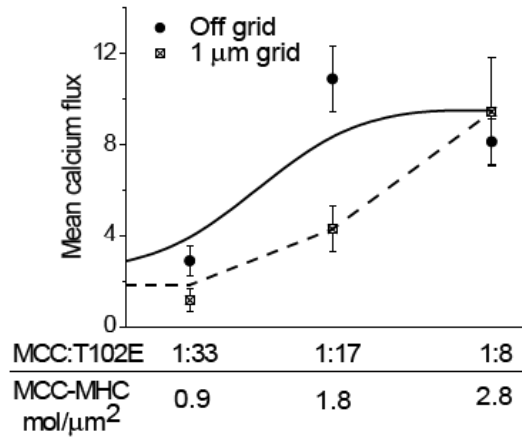


Supplementary figure 4.

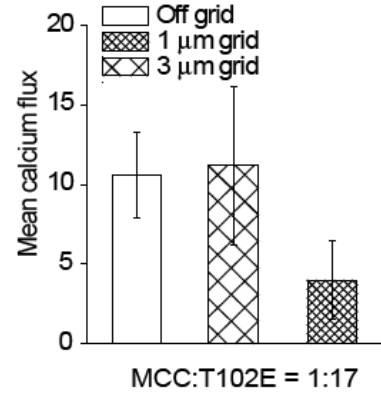


**Supplementary figure 5.**

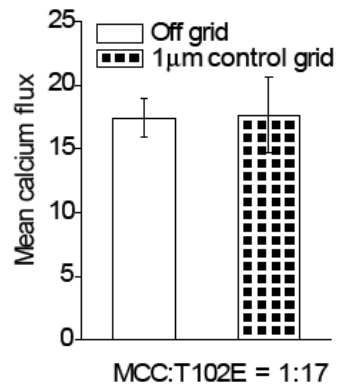
**a**



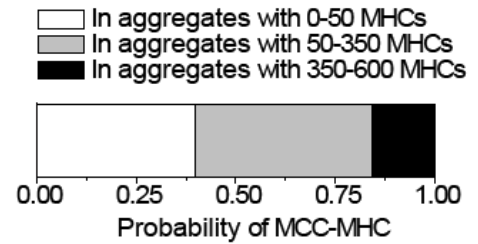
**b**



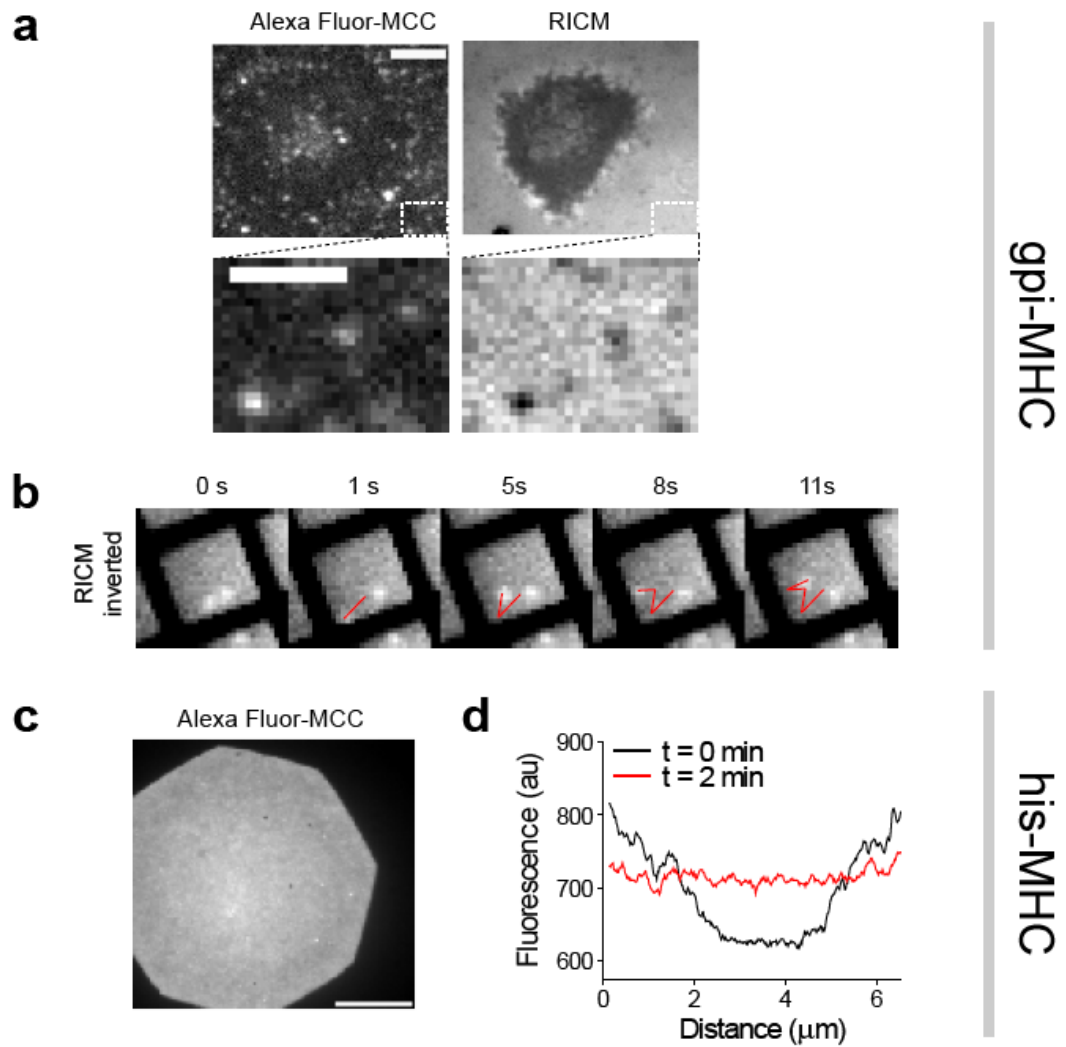
**c**



**d**



## Supplementary figure 6.



## **Disclaimers**

This document was prepared as an account of work sponsored by the United States Government. While this document is believed to contain correct information, neither the United States Government nor any agency thereof, nor the Regents of the University of California, nor any of their employees, makes any warranty, express or implied, or assumes any legal responsibility for the accuracy, completeness, or usefulness of any information, apparatus, product, or process disclosed, or represents that its use would not infringe privately owned rights. Reference herein to any specific commercial product, process, or service by its trade name, trademark, manufacturer, or otherwise, does not necessarily constitute or imply its endorsement, recommendation, or favoring by the United States Government or any agency thereof, or the Regents of the University of California. The views and opinions of authors expressed herein do not necessarily state or reflect those of the United States Government or any agency thereof or the Regents of the University of California.

## **Copyright notice**

This manuscript has been authored by an author at Lawrence Berkeley National Laboratory under Contract No. DE-AC02-05CH11231 with the U.S. Department of Energy. The U.S. Government retains, and the publisher, by accepting the article for publication, acknowledges, that the U.S. Government retains a non-exclusive, paid-up, irrevocable, world-wide license to publish or reproduce the published form of this manuscript, or allow others to do so, for U.S. Government purposes.